View metadata, citation and similar papers at core.ac.uk

brought to you by CORE

provided by Royal Holloway - Pure

The Plant Cell, Vol. 16, 643–657, March 2004, www.plantcell.org © 2004 American Society of Plant Biologists

Expression of a Nondegradable Cyclin B1 Affects Plant Development and Leads to Endomitosis by Inhibiting the Formation of a Phragmoplast

Magdalena Weingartner,[a] Marie-Claire Criqui,[b] Tamás Mészáros,[c] Pavla Binarova,[d] Anne-Catherine Schmit,[b] Anne Helfer,[c] Aude Derevier,[b] Mathieu Erhardt,[b] László Bögre,[c] and Pascal Genschik[b,1]

[a] Max Planck Institute of Molecular Plant Physiology, 14476 Golm, Germany
[b] Institut de Biologie Moléculaire des Plantes du Centre National de la Recherche Scientifique, 67084 Strasbourg Cédex, France
[c] School of Biological Sciences, Royal Holloway College, University of London, Egham, Surrey TW20 OEX, United Kingdom
[d] Institute of Microbiology, Academy of Sciences of the Czech Republic, 142 20 Prague 4, Czech Republic

In plants after the disassembly of mitotic spindle, a specific cytokinetic structure called the phragmoplast is built, and after cytokinesis, microtubules populate the cell cortex in an organized orientation that determines cell elongation and shape. Here, we show that impaired cyclin B1 degradation, resulting from a mutation within its destruction box, leads to an isodiametric shape of epidermal cells in leaves, stems, and roots and retarded growth of seedlings. Microtubules in these misshaped cells are grossly disorganized, focused around the nucleus, whereas they were entirely missing or abnormally organized along the cell cortex. A high percentage of cells expressing nondestructible cyclin B1 had doubled DNA content as a result of undergoing endomitosis. During anaphase the cytokinesis-specific syntaxin KNOLLE could still localize to the midplane of cell division, whereas NPK1-activating kinesin-like protein 1, a cytokinetic kinesin-related protein, was unable to do so, and instead of the formation of a phragmoplast, the midzone microtubules persisted between the separated nuclei, which eventually fused. In summary, our results show that the timely degradation of mitotic cyclins in plants is required for the reorganization of mitotic microtubules to the phragmoplast and for proper cytokinesis. Subsequently, the presence of nondegradable cyclin B1 leads to a failure in organizing properly the cortical microtubules that determine cell elongation and shape.

INTRODUCTION

The sequential waves of the different cyclin–cyclin-dependent kinase (CDK) activities regulate the progress through cell cycle phases, and a major component behind this oscillation is the timed expression and degradation of cyclins (Pines and Rieder, 2001). In mammals, two B-type cyclins (B1 and B2) have been identified so far (Minshull et al., 1989; Pines and Hunter, 1989), whereas chickens, frogs, flies, and worms possess a third B-type cyclin called B3 (Gallant and Nigg, 1994; Kreutzer et al., 1995). The activation of cyclin B/CDK1 kinase complex triggers entry into mitosis. How various B-type cyclins function and confer specificity to CDKs is not fully understood, but evidence points to specific subcellular localization of the cyclin-CDK complexes and/or substrate preferences. This is supported by B-type cyclin localization studies (reviewed in Pines, 1999; Yang and Kornbluth, 1999; Jackman et al., 2003). It has been proposed that the role of cyclin B1/CDK1 kinase is to phosphorylate and disassemble the nuclear lamina to promote nuclear envelope breakdown (Li et al., 1997, Nigg, 2001). In addition, cyclin B-CDK1 kinase has also been documented to be involved in mitotic chromosome condensation (Kimura et al., 1998; reviewed in Uhlmann, 2001) and to control microtubule (MT) dynamics during mitosis via phosphorylation of MT-associated proteins (Vasquez et al., 1999).

However, it has been well established in fungi and animals that CDK activities need to be switched off during mitotic exit for spindle disassembly, cytokinesis, and licensing of replication origins during G1, which is necessary for a novel round of DNA synthesis (reviewed in Zachariae and Nasmyth, 1999). CDK inactivation is believed to occur essentially through proteolysis of the B-type cyclins by a multisubunit ubiquitin protein ligase, termed the anaphase-promoting complex or cyclosome (APC/C) (reviewed in Harper et al., 2002; Peters, 2002). B-type cyclin degradation is dependent on a specific sequence element in its N-terminal region, termed the destruction box (D-box) (Glotzer et al., 1991). CDK inhibitor (CKI) proteins also participate in CDK inactivation during mitosis in both *Saccharomyces cerevisiae* (yeast) and *Drosophila melanogaster* (Foley and Sprenger, 2001; Irniger, 2002).

The first demonstration that cyclin B degradation is required for mitotic exit was obtained with *Arbacia punctulata* (sea urchin) cyclin B (Murray et al., 1989). These authors showed that an N-terminal truncated version of the protein that was stable,

[1] To whom correspondence should be addressed. E-mail pascal.genschik@ibmp-ulp.u-strasbg.fr; fax 33 (0)3 88 61 44 42.
The author responsible for distribution of materials integral to the findings presented in this article in accordance with the policy described in the Instructions for Authors (www.plantcell.org) is: Pascal Genschik (pascal.genschik@ibmp-ulp.u-strasbg.fr).
Article, publication date, and citation information can be found at www.plantcell.org/cgi/doi/10.1105/tpc.020057.

maintained strong CDK activity, and arrested the frog eggs in meiosis and, when fertilized, in mitosis. The nondegradable cyclin was unable to block sister chromatid separation, but subsequently chromosomes could not decondense, and the nuclear envelopes did not reassemble (Holloway et al., 1993). Nondegradable versions of mitotic cyclins also produced a mitotic arrest in *D. melanogaster* (Rimmington et al., 1994; Sigrist et al., 1995) and HeLa cells (Gallant and Nigg, 1992). In *S. cerevisiae* (budding yeast), high levels of nondegradable cyclin CLB2 arrest cells late in mitosis, with segregated chromosomes and the presence of an elongated mitotic spindle (Surana et al., 1993). Indestructible cyclin Cdc13 arrests *Schizosaccharomyces pombe* cells in anaphase with separated and condensed chromosomes and no septa (Yamano et al., 1996).

However, in these different studies, the mitotic cyclins were expressed at high levels, well above the endogenous cyclin levels. In *S. cerevisiae* it was shown that the expression of nondegradable cyclin CLB2 at a modest level (Amon et al., 1994) or under the control of the CLB5 promoter (Cross et al., 1999) does not lead to mitotic arrest. Nevertheless, when the nondegradable cyclin CLB2 is under the control of its own promoter, the overexpression of the CKI substrate/subunit inhibitor of cyclin-dependent kinase is required to maintain the *S. cerevisiae* cells viable (Wäsch and Cross, 2002).

In plants, the functions of the different mitotic cyclins, their subcellular localizations, as well as their stabilities during the cell cycle are only poorly understood (Criqui and Genschik, 2002). We have previously demonstrated in synchronized *Nicotiana tabacum* (tobacco) BY2 cells that endogenous cyclin B1;1 protein undergoes cell cycle–dependent proteolysis and is stabilized after proteasome inhibitor treatment (Criqui et al., 2000). Furthermore, by recording time-lapse images of BY2 cells expressing different *N. tabacum* cyclin B1-GFP (green fluorescent protein) fusion proteins under the control of a dexamethasone (Dex)-inducible promoter, we found that cyclin degradation started at the onset of anaphase and occurred most likely at close proximity to the chromosomes (Criqui et al., 2001). The proteolysis of a B2-type cyclin in early mitosis has also been reported recently (Weingartner et al., 2003). Surprisingly, the degradation of the B2-type cyclin at prometaphase is proteosome independent. Immunolocalization experiments performed in maize (*Zea mays*) root tip cells indicated that several mitotic cyclins were not destroyed at the exit of mitosis, although these proteins carry a D-box (Mews et al., 1997). Thus, the necessity to destroy mitotic cyclins during plant mitosis is still under debate (Mironov et al., 1999; Capron et al., 2003). Furthermore, plant mitosis has several particular features not shared in other organisms, among them the complexity of the cyclin gene family, which is much higher in plants than in animals (the genome of Arabidopsis encodes not <10 A-type and nine B-type cyclins; see Vandepoele et al., 2002), and the presence of MT arrays, such as cortical MTs, the preprophase band (PPB), and the phragmoplast, which are unique to plants (reviewed in Azimzadeh et al., 2001). Here, we investigate the importance of the timely degradation of cyclin B1 during the cell cycle–phase-specific interchange of these MT structures and the consequences of accumulating high levels of nondegradable cyclin B1 on plant development.

RESULTS

Constitutive Overexpression of Nondegradable Cyclin B1 in Transgenic *N. tabacum* Plants

To examine the effects of nondegradable cyclin on plant growth and development, we engineered two constructs in which either the native cyclin B1;1 (pBi:CycB1myc) or the nondegradable cyclin B1;1 (pBi:ΔD-boxCycB1myc) coding sequences were myc-tagged at the C terminus and put under the control of the strong and constitutive 35S promoter of the *Cauliflower mosaic virus*. Oligonucleotides that specifically amplify the nondegradable and native cyclins were designed to detect the mRNA product (Figure 1A).

N. tabacum plants were either transformed with the cyclin constructs or with the pBI:GUS control construct, in which the cyclin sequence was replaced by the β-glucuronidase (*GUS*) protein. Ten independent transformants expressing the myc-tagged native cyclin, based on reverse transcription (RT)–PCR analysis, and 10 independent transformants expressing the *GUS* gene were selected. Compared with the pBi:CycB1myc and pBI:GUS constructs, the transformation with the nondegradable cyclin construct was poorly efficient, but 10 independent transformants could finally be recovered (called CycB1Mut1-to-10). One of these plants, CycB1Mut8, was not fertile and thus was not studied further. The other nine CycB1Mut plants were self-pollinated, and segregation analyses indicated a variable number of integrations, ranging from one to at least three. Six different T1 plants (called lines I to VI) for each CycB1Mut line were further analyzed for transgene expression by RT-PCR (Figure 1B) and RNA gels (Figure 1C). Out of these 54 T1 plants analyzed, only three T1 plants from line CycB1Mut5 (I, II, and V) and four T1 plants from line CycB1Mut6 (I, II, III, and V) showed expression of the transgene, as shown for lines CycB1Mut5-I and CycB1Mut6-I (Figures 1B to 1D). For all the other lines, we observed either no expression or the expression of a truncated version of the cyclin B1, as illustrated for line CycB1Mut5-IV (Figures 1B and 1C, lane 2). Truncated versions of the cyclin B1 were also found in the T1 progeny of lines CycB1Mut1, CycB1Mut2, and CycB1Mut4 (data not shown). The reasons for these rearrangements of the transgene are not clear, and these plants were not further characterized.

Strikingly, all the plants expressing the transgene exhibited asymmetric and blistered leaves (as shown for plant CycB1-Mut5-I in Figures 1F to 1H). We believe that this phenotype is the consequence of nondegradable cyclin expression because it was never observed in the pBi:CycB1myc lines, the pBI:GUS control lines, or the CycB1Mut lines that do not express the transgene. Further evidence for this comes from the line CycB1-Mut5 that integrated two copies of the transgene, one producing a truncated version of the nondegradable cyclin and the other producing the full-length transcript (Figures 1B and 1C). Only the T1 plants segregating the transgene that expresses the full-length transcript presented the phenotypes (Figures 1E to 1H).

In addition to the phenotypes described above, progeny T1 plants of line CycB1Mut6 were more severely affected (Figure 1I). Those plants showed a stronger leaf phenotype affecting both leaf lamina and margin and, in the most severe cases, producing

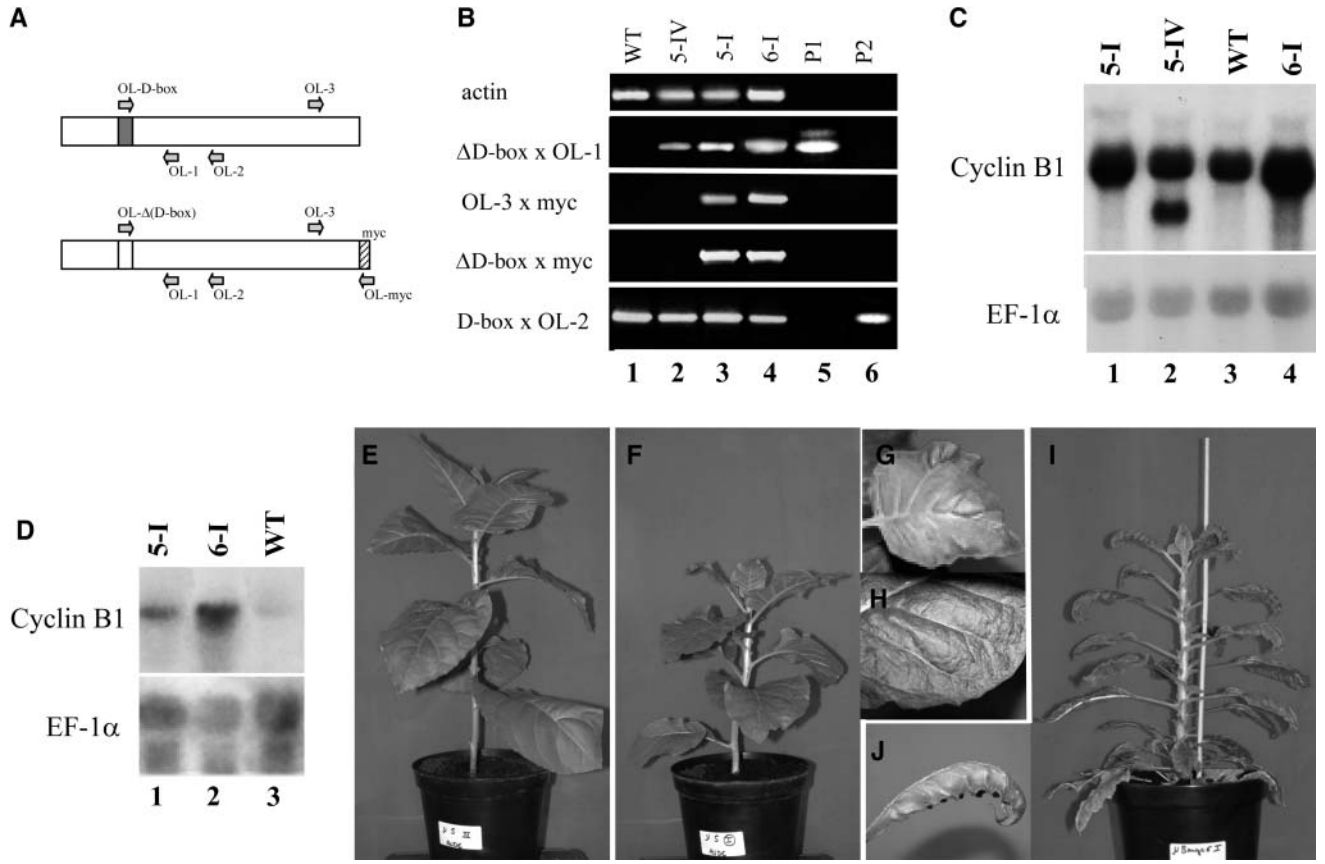

Figure 1. Cyclin B1 Expression and Phenotypic Analysis of the T1 Transgenic Plants.

(A) Schematic representation of the native and transgenic nondegradable cyclin B1 and positions of the PCR primers. The shaded box indicates the native D-box sequence, and the hatched box represents the myc sequence.

(B) RT-PCR analysis of cyclin B1 transcript accumulation in untransformed wild-type and progeny T1 plants of CycB1Mut5 (5-IV [lane 2] and 5-I [lane 3]) and CycMut6 lines (6-I [lane 4]). P1 (lane 5) and P2 (lane 6) correspond to PCR control reactions realized on plasmids pSKCycBMutD-box-CAT (P1) and pSKCycB-CAT (P2) described in Genschik et al. (1998).

(C) and **(D)** RNA gel blot analysis of leaf extracts from wild-type and progeny T1 plants from the CycB1Mut5 (5-I and 5-IV) and CycMut6 (6-I) lines. Samples were taken at two different developmental stages; leaves <3 cm in length containing high cell division activity **(C)** and expanding leaves >10 cm in length **(D)**. Twenty micrograms of total RNA were separated by electrophoresis on an agarose-formaldehyde gel, transferred to a nylon membrane, and hybridized successively with the indicated probes.

(E) to **(H)** Forty-five-day-old soil-grown plant, lines CycB1Mut5-IV **(E)** and CycB1Mut5-I **(F)**. At this stage of development, the CycB1Mut5-I plant developed already asymmetric and blistered leaves (**[G]** to **[H]**).

(I) and **(J)** Six-month-old soil-grown plant, line CycB1Mut6-I **(I)** exhibiting serrated and curled leaves **(J)**.

narrow serrated leaves (Figure 1J). In addition, the plants also exhibited severe growth retardation. Interestingly, these plants showed the highest expression levels of the transgene (as shown for line CycB1Mut6-I in Figures 1C and 1D), showing a correlation between the level of expression and the severity of the phenotypes. Most of the CycB1Mut6 lines were poorly fertile and produced a reduced number of seeds.

Altered Morphology and Increased Ploidy in Seedlings Deriving from Lines CycB1Mut6-I and CycB1Mut6-III

Seedlings deriving from lines CycB1Mut6-I and CycB1Mut6-III are severely delayed in growth and have postembryonic defects in the apical part (cotyledon and leaves), in the hypocotyl, and in the root. The morphological defects can be classified into three major groups. The less severe abnormalities observed (which represent 11% of the seedlings) affect mainly the development of cotyledons (Figure 2A), which do not expand to their full size and their epidermal pavement cells are irregular in shape, as observed by environmental scanning electron microscopy (Figure 2B). However, these plantlets develop normal leaves.

The second group of seedlings, by far the most frequent (76% of the seedlings), is severely affected in development and morphogenesis. These seedlings develop shrunken and stunted cotyledons that do not turn green and have epidermal cells with irregular shape (Figure 2C). Longitudinal sections through the

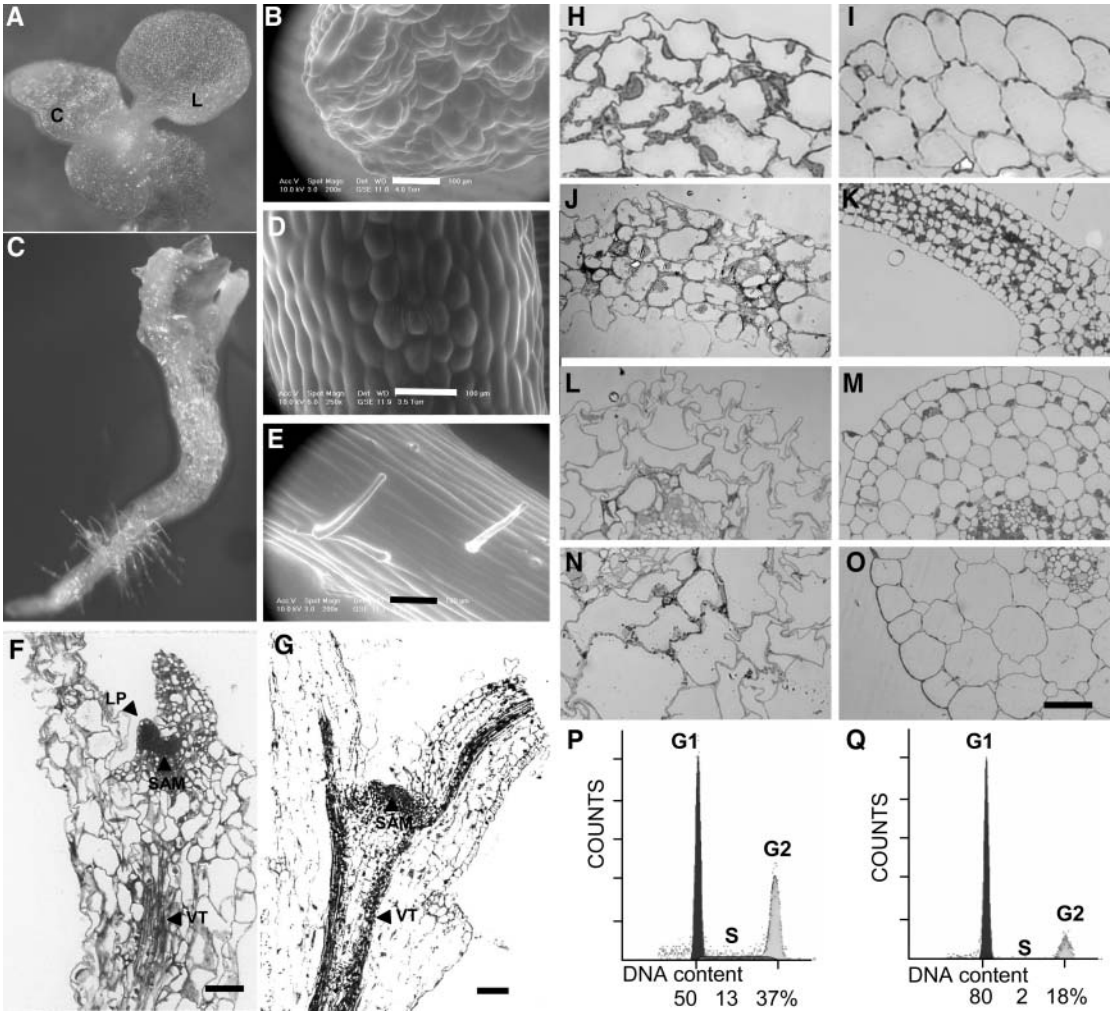

Figure 2. Ectopic Nondegradable Cyclin B1 Expression Affects *N. tabacum* Seedling Development.

(A) and **(C)** Appearance of 20-d-old seedlings germinated on plant agar deriving from lines CycBMut6-I. C, cotyledon; L, leaf.

(B), **(D)**, and **(E)** Environmental scanning electron micrographs showing abnormalities in cotyledon of weakly affected offsprings from line CycB1Mut6-I **(B)** and in the epidermal cell layer of a bulging hypocotyl of severely affected 10-d-old offspring from line CycB1Mut6-I **(D)** compared with a normal growing pBI:GUS transgenic *N. tabacum* seedling **(E)**.

(F) and **(G)** Longitudinal sections through a paraffin-embedded seedling from line CycB1Mut6-III **(F)**, which has a similar phenotype like that shown in **(C)** and from the pBI:GUS transgenic control line **(G)**. LP, leaf primordial; SAM, shoot apical meristem; VT, vascular tissue.

(H) to **(O)** Sections of seedlings deriving from line CycB1Mut6-I, which are similar to that shown in **(C)** (see **[H]**, **[J]**, **[L]**, and **[N]**), and of a transgenic control seedling harboring a pBI:GUS construct (see **[I]**, **[K]**, **[M]**, and **[O]**). Young leaves (**[H]** and **[I]**), petioles (**[J]** and **[K]**), hypocotyls (**[L]** and **[M]**), and roots (**[N]** and **[O]**) are shown.

(P) and **(Q)** Histograms of the DNA distribution in CycB1Mut6-I transgenic T2 seedlings 20 d after germination **(P)** compared with the pBI:GUS transgenic *N. tabacum* seedling from the same age **(Q)**. Percentage of cell cycle distribution of the nuclei is mentioned below. Bars = 100 μM in **(B)** and **(D)** to **(G)**, and 200 μM in **(H)** to **(O)**.

seedlings show that the shoot apical meristem is present, although of abnormal shape (Figure 2F), as compared with control seedlings of the same age (Figure 2G). Nevertheless, the meristem remains functional because young leaf primordia can emerge but never fully expand in size (Figures 2C and 2F).

This second group is also affected at the hypocotyl level, which is bulging (Figure 2C). A closer inspection reveals that the epidermal cells do not elongate (Figure 2D) compared with a normally growing *N. tabacum* seedling (Figure 2E), and no hairs can be observed on the hypocotyl epidermal cell layer. These two characteristics indicate that the plants are impaired in the process of cell differentiation. Thus, inhibition of cell elongation produced the radial swelling of hypocotyls.

Strikingly, further analysis of this class of seedlings showed that cells in various tissues have irregular shapes (Figures 2H, 2J, 2L, and 2N) compared with a control seedling (Figures 2I, 2K, 2M,

and 2O). Except in the young leaf (Figures 2H and 2I), many cells are in general larger in size, like in petiole (Figures 2J and 2K), hypocotyl (Figures 2L and 2M), and root (Figures 2N and 2O). Immunodetection with the anti-cyclin B1 antibody (data not shown) revealed that these seedlings expressed high levels of the transgene. Finally, a third group can be defined (the remaining seedlings), in which seedling development is even more severely affected, leading to seedling lethality at ~14 d after germination (data not shown).

Flow cytometry analysis used to determine the DNA content in the seedling of the second group revealed a higher percentage of cells with a duplicated ploidy level (Figure 2P) compared with the control seedlings (Figure 2Q). However, larger DNA content than 4C has not been found, indicating that endoreduplication is not happening in these cells.

The Nondestructible Cyclin B1 Expression Leads to Abnormal Mitosis in Seedlings

To further analyze the cellular abnormalities in the *N. tabacum* seedling expressing the nondestructible CycB1Mut, we performed immunostaining for α-tubulin in seedlings belonging to the second group (see above) and in pBI:GUS control seedlings 8 d after germination. The nuclear material was stained with 4′,6-diamidino-2-phenylindole (DAPI). Although the epidermal cells in the root and the hypocotyl did not elongate and exhibit an irregular shape (Figure 2D), these cells were mainly mononucleated with cortical MTs oriented perpendicular to the growth axis, as observed in the wild type and control transgenic seedlings (data not shown). However, both cortical and endodermal cells in the hypocotyl and root were more severely affected, and we observed different abnormalities in the organization of the MTs and the nuclear material. In contrast with the control line (Figure 3A), cortical MTs from the line expressing the mutated cyclin B1 were often oriented parallel to the growth axis (Figure 3B) or were randomly distributed (data not shown). Furthermore, in many mononucleated cells, we noticed the presence of condensed chromatin, and the cortical MTs were either nonexistent or their numbers dramatically reduced. In such cells, MTs seem to irradiate from the nuclear periphery (Figure 3C).

In the root apex, up to 37% of the cells contained micronuclei more or less associated with short remnant MT bundles or rings (Figure 3D). Some cells in the root meristem were observed in a telophase-like stage, but they did not develop a phragmoplast, and the two daughter nuclei remained close to each other (10% of 500 cells observed) (Figure 3E). In other cells the two nuclei seem to stick together and are surrounded by disorganized MTs emanating from the nuclear periphery (Figure 3F), suggesting that ectopic stable cyclin B1 expression interferes with cell plate formation and mitotic exit leading to endomitosis or to polyploidization. This finding was supported by flow cytometry analysis used to determine the DNA content (Figure 2P).

To investigate more specifically how nondegradable cyclin B1 expression interferes with cell cycle progression and mitosis, we used the highly synchronizable *N. tabacum* BY2 cell line (Nagata et al., 1992) with a chemically inducible expression of a CycB1Mut-GFP fusion protein.

High Expression of Nondegradable Cyclin B1 Impairs Mitosis after Metaphase, whereas CDK Activity Is Only Transiently Elevated

We established clonal cell suspension cultures with the pTA:CycB1;1(ΔD-box)-GFP vector (Criqui et al., 2001), in which the transgene is under the control of the Dex-inducible promoter (Aoyama and Chua, 1997). Two of these cell lines (called CycBMut-GFP-3 and CycBMut-GFP-10) were selected for having higher expression levels of the transgene than those described previously (Criqui et al., 2001). As a control, we used a pTA:GFP cell line expressing high levels of the GFP protein from the same promoter.

Based on the analyses of the transgenic plants (see above), the overexpression of the nondegradable cyclin B1 should lead to higher ploidy levels. Therefore, we analyzed by flow cytometry the DNA contents of both CycBMut-GFP-3 and GFP cell lines before and after Dex induction (Figures 4A and 4B). When grown asynchronously without Dex treatment, both cell suspension cultures contained a similar DNA content with ~80% 2C and 15% 4C cells. When the expression of the GFP alone was induced for a period of 16 h, no major change in DNA content was found (Figure 4A). However, when the nondegradable cyclin B1 was induced, a strong reduction in the number of 2C cells and a higher value of 4C cells was observed (Figure 4B).

To address the consequences of nondestructible cyclin B1 expression on cell cycle progression, we synchronized the cell suspension cultures by aphidicolin treatment, which blocks cell cycle progression specifically during S phase. Under these conditions, cells expressing the nondegradable cyclin B1 entered mitosis at a similar rate as control cells expressing GFP alone (data not shown). Thus, the nondegradable cyclin has no or only limited effects on S-phase progression and on the G2-to-M transition.

Whereas Dex-induced cells expressing the GFP protein or noninduced CycBMut-GFP control cells progressed through mitosis normally, most of the cells expressing the nondegradable cyclin B1 were arrested or severely delayed in their mitotic progression (Figure 4C, top). We measured histone H1 kinase activity in immunoprecipitates specific to A-type CDKs and found a prolonged and increased CDK activity in the induced cells compared with the control cells (Figure 4C, bottom). However, at the 16-h time point, the CDK activity did start to decline.

To specifically investigate the effect of the indestructible cyclin on the exit from mitosis, we synchronized cells for metaphase by a sequential release from aphidicolin-induced S phase and propyzamide-induced prometaphase blocks (Figure 4D, top). A similar number of Dex-induced and noninduced cells reached the prometaphase stage, indicating that the nondegradable cyclin B1 does not affect mitotic entry. After removal of propyzamide, most noninduced cells finished mitosis within 3 to 4 h, whereas a high percentage of the cells expressing the mutated cyclin B1 were still in mitosis. Histone H1 kinase activities were

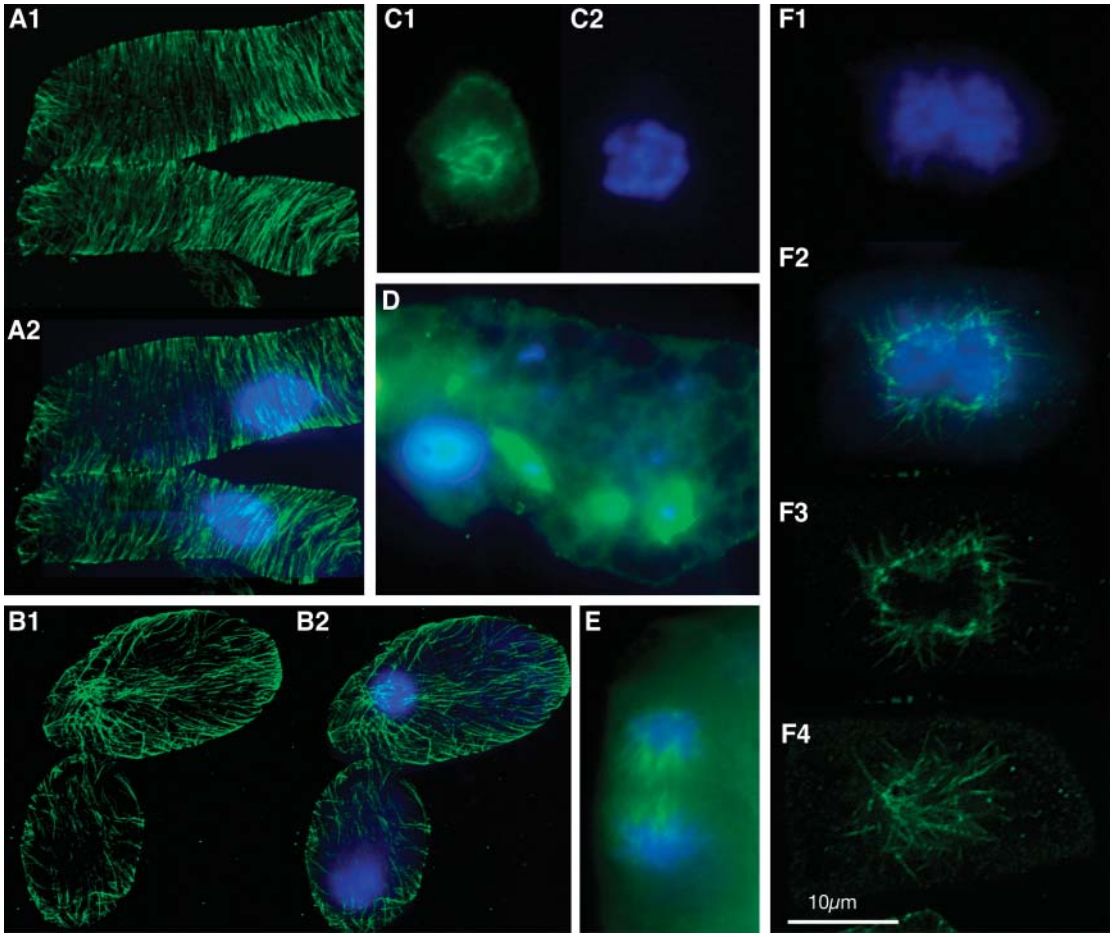

Figure 3. Seedlings Overexpressing Nondegradable Cyclin B1 Exhibit Abnormal MT Arrays and Mitotic Figures.

(A) Immunostaining of α-tubulin in root cells from a pBI:GUS control seedling observed by confocal microscopy. The image (A2) is a merged picture showing α-tubulin (green) and chromatin stained by DAPI (blue).

(B) Immunostaining of α-tubulin in root cells of seedlings deriving from the CycB1Mut6-III line observed by confocal microscopy. The image (B2) is a merged picture showing α-tubulin (green) and chromatin stained by DAPI (blue).

(C) and **(D)** Merged images of immunostaining for α-tubulin (green) and chromatin staining by DAPI (blue) in root tip cells of seedlings deriving from the CycB1Mut6-III line showing condensed chromatin in mononucleated cells **(C)** or micronuclei **(D)** as well as abnormal MT arrays.

(E) Merged image of immunostaining for α-tubulin (green) and chromatin staining by DAPI (blue) in root meristematic cells of seedlings in a telophase-like stage deriving from the CycB1Mut6-III line.

(F) Root cells from CycB1Mut6-III transgenic T2 seedlings in a pseudo-G1 stage, in which the two daughter nuclei seem to stick together. The merged image (F2) is of DAPI (F1) and α-tubulin (F3) staining observed by confocal microscopy. Image (F4) is a focal plane showing MTs emanating from the nuclear material. Bar = 10 μM.

measured upon $p9^{CksHs1}$ affinity purification, and we observed again a transient increase in CDK-kinase activities (Figure 4D, bottom) in cells expressing the mutated cyclin B1.

It is not established whether cyclin B1 is in complex with A- or B-type CDKs. We decided to examine this issue in Arabidopsis, in which cell cycle components are most comprehensively known (Vandepoele et al., 2002) and specific antibodies were available for Arath;*CDKA;1* and Arath;*CDKB1;1*. We prepared a construct in which the Arabidopsis cyclin B1;1 (Arath;*CYCB1;1*) was His-tagged and cloned into a vector suitable for in vitro translation and expressed either alone or together with the Arath;*CDKA;1* or Arath;*CDKB1;1* in wheat germ extracts. In vitro pull-down assays using Ni-agarose beads showed that Arath;*CYCB1;1* could interact both with A- and B-type CDKs (Figure 4E). Moreover, we detected histone H1 kinase activity in the affinity-purified protein fractions (Figure 4F). The weak kinase activity present when only cyclin B1 was translated suggests that the cyclin B protein interacted with CDKs present in the wheat germ extract. However, a much stronger activity was present when either Arath;*CDKA;1* or Arath;*CDKB1;1* was cotranslated. From these experiments we conclude that cyclin B1 is able to bind and activate both A-type and B-type CDKs, at least in vitro.

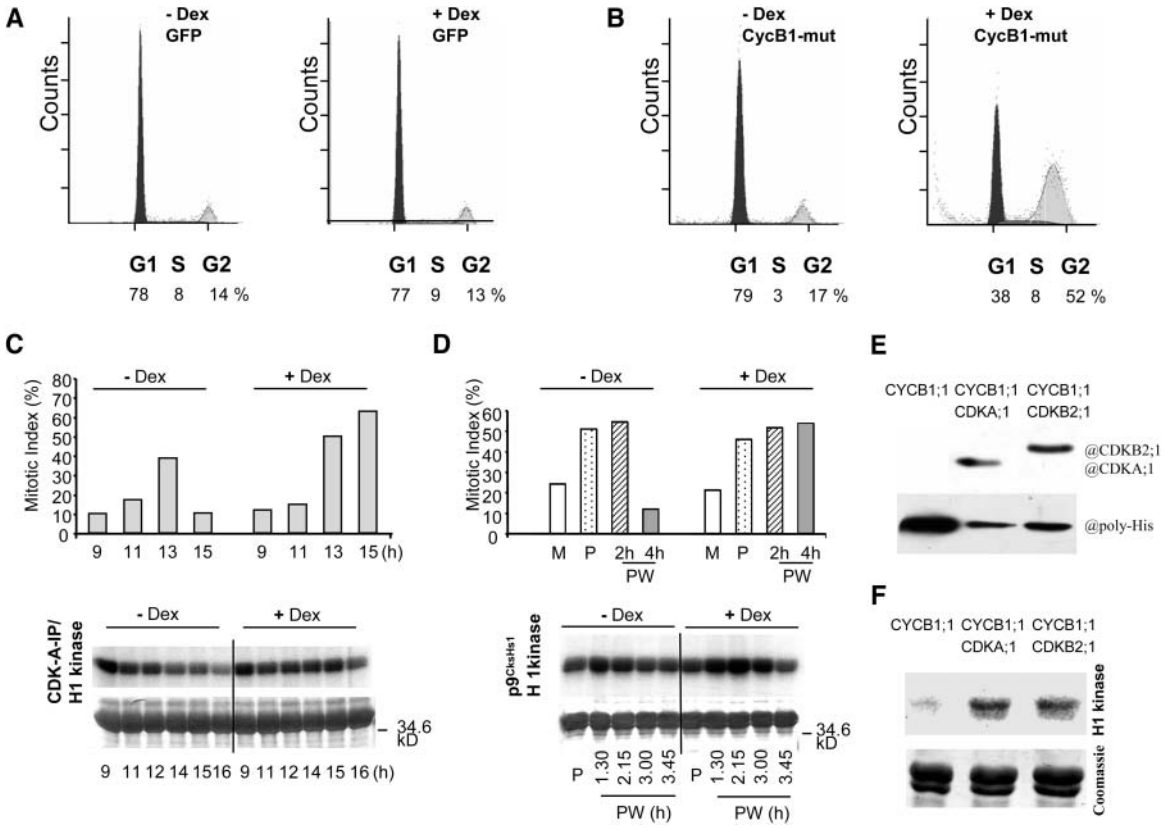

Figure 4. Ectopic Expression of Nondegradable Cyclin B1-GFP Produces Higher Ploidy Level and Leads to an Elevated Mitotic Kinase Activity during Late Mitotic Stages in Synchronized BY2 Cells.

(A) and **(B)** Flow cytometry measurements of G1 and G2 DNA contents in isolated nuclei from the *N. tabacum* BY2 GFP **(A)** and CycBMut-GFP-3 **(B)** cell lines grown asynchronously before (−Dex) and 16 h after (+Dex) Dex induction.

(C) Cells were synchronized with aphidicolin and incubated without (−Dex) or with Dex (+Dex) to induce nondegradable cyclin B1-GFP expression. Samples were taken during G2 phase (9 h) and mitotic stages (11 to 15 h). Mitotic indices in samples taken at 9, 11, 13, and 15 h after aphidicolin release (top). Histone H1 associated kinase activity measured in CdkA-bound immunoprecipitates from protein extracts prepared from samples taken at 9, 11, 12, 14, 15, and 16 h after aphidicolin release (bottom).

(D) Cells were synchronized with aphidicolin and incubated without (−Dex) or with dexamethasone (+Dex) to induce nondegradable cyclin B1-GFP expression. At 7 h after the aphidicolin release, cells were treated for 6 h with propyzamide, which blocked cells in prometaphase. After propyzamide washout, samples were taken at indicated time points. Mitotic indices measured in samples taken during mitosis at 12 h after aphidicolin release (top) without propyzamide treatment (M), during propyzamide block at 13 h after aphidicolin release (P), and at 2 and 4 h after propyzamide washout. Histone H1–associated kinase activity measured in $p9^{CksHs1}$ affinity purified protein fractions from propyzamide blocked cells and from cells at 1.30, 2.15, 3 and 3.45 h after propyzamide release (bottom).

(E) and **(F)** Interaction and activity of in vitro translated Arabidopsis cyclin B1 and Cdks. The translated proteins were mixed and purified with His-agarose beads. The purified extracts were resolved on 10% PAGE, blotted, and probed with the poly-His and Cdk specific antibodies, as indicated **(E)**. The same protein mixtures were analyzed by in vitro kinase assays using histone H1 as a substrate **(F)**.

Nondegradable Cyclin B1 Impairs Plant Cytokinesis and Results in Endomitosis

To understand how the expression of the nondestructible cyclin B1 alters mitotic progression, time-lapse analyses of mitosis were performed. As we have reported previously, cyclin B1 binds to the nuclear material from early prophase and becomes destroyed in metaphase (Criqui et al., 2001). Because the nondestructible cyclin B1 remains associated with the chromosomes until the end of mitosis and the next G1 phase, we were able to visualize chromosome movements throughout mitosis in live cells in the CycBMut-GFP culture. Time-lapse image recording revealed that most of the cells progressed normally through prophase and metaphase and initiated chromosome segregation but arrested transiently in a telophase-like stage, in which the two separated sets of chromatin were overcondensed and abnormally round shaped. In most cases, these nuclear materials finally fused together (as shown in Figure 5A). Because these cells initiated anaphase but lacked nuclear division and cytokinesis, we considered this process as similar to endomitosis (reviewed in Edgar and Orr-Weaver, 2001). However, sometimes the defective

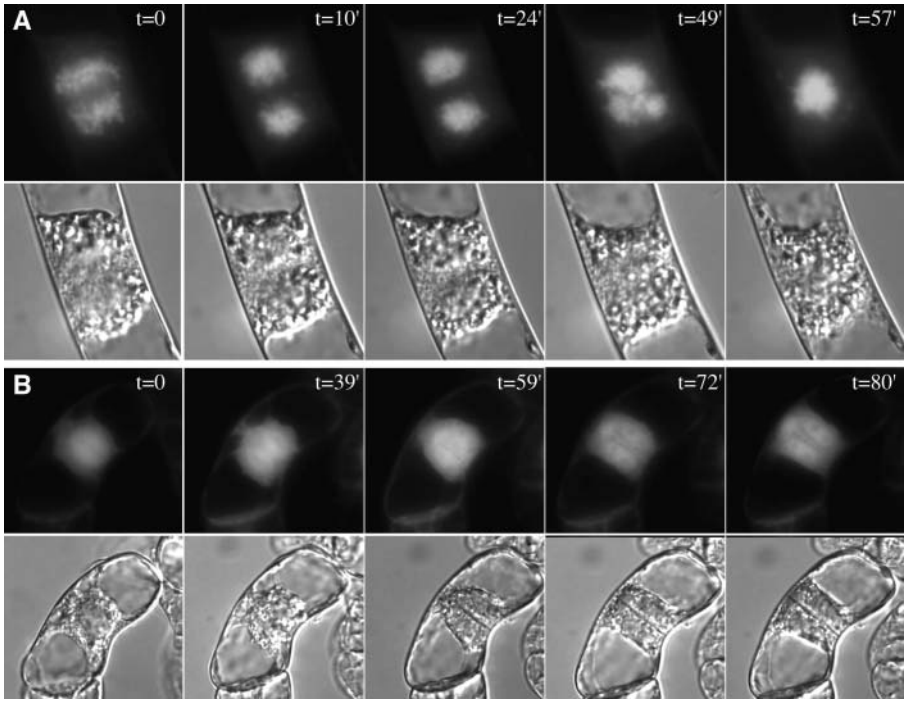

Figure 5. Ectopic Expression of CycBMut-GFP Interferes with Cytokinesis, whereas Expression of GFP Alone Does Not Affect Mitotic Progression.

(A) and **(B)** Time-lapse images of living cells expressing the nondegradable cyclin B1;1-GFP fusion protein **(A)** or the GFP protein alone **(B)** from a Dex-inducible promoter during progression through anaphase, telophase, and cytokinesis. Fluorescent images shown at top, and the corresponding differential interference contrast images shown at bottom.

cytokinesis led also to the formation of polynucleated cells with two or more nuclei of unequal size (data not shown). By contrast, the control cells expressing GFP alone progressed normally from metaphase through anaphase, telophase, and cytokinesis (Figure 5B).

The Organization of Phragmoplast MTs Is Impaired When Cyclin B1 Is Not Destroyed after Metaphase

To learn more about the abortive cytokinesis in the cells expressing the nondegradable cyclin B1, we performed immunostaining for α-tubulin. In noninduced CycBMut-GFP control cells or in Dex-induced cells expressing the GFP alone, all mitotic MT arrays, including the PPB, metaphase and anaphase spindles, and the phragmoplast were detected at the expected frequency (Figure 6A, top). In Dex-induced cells expressing CycBMut-GFP, the presence of the PPB in late G2 phase indicated that the nondegradable cyclin B1 had no apparent effect on the G2-to-M transition (data not shown). These cells also developed normally shaped metaphase spindles (Figure 6A, Meta). However, in contrast with the noninduced cells, a reduction of MT labeling in the midzone of the elongating anaphase spindle was frequently observed (Figure 6A, Ana, left) as well as cells in which the MTs of the midzone spindle were entirely missing, whereas the kinetochore MTs at the poles were detectable and tightly linked to separating chromatids (Figure 6A, Ana, right). Finally, in cells at a stage corresponding to telophase, the MTs, instead of forming the phragmoplast, were tightly associated in the form of unorganized arrays with separated chromatids, still highly condensed but forming round shaped masses (Figure 6A, Telo). These two sets of chromatids were later fused to a single nucleus in G1 phase–like stage (Figure 6A, Cytkin). Frequently these cells displayed many abnormalities of microtubular cytoskeleton arrangement. The regular pattern of cortical MT arrangement was disturbed, and in some cases cortical MTs were absent. Thus, the sustained overexpression of stable cyclin B1 interferes also with proper organization of the cortical MTs during the next G1 phase.

KNOLLE, but Not NACK1, Is Still Able to Localize to the Midplane of Abnormal Anaphase Spindles

To understand how the anaphase spindle is destabilized in cells in which Cyclin B1 is not destructed, we investigated the localization of proteins known to be present and important at the site of cell plate formation; these were the cytokinesis-specific syntaxin KNOLLE (Lauber et al., 1997) and the cytokinesis-specific kinesin NPK1-activating kinesin-like protein 1 (NACK1) (Nishihama et al., 2002). Double immunofluorescence labeling for α-tubulin and KNOLLE in cells in which CycB1Mut expression was not induced indicated the expected localization of the KNOLLE protein to the midzone of the anaphase spindle and to the phragmoplast (Figure 6B). In the presence of Dex, the signal for KNOLLE immunolabeling was still enriched on the

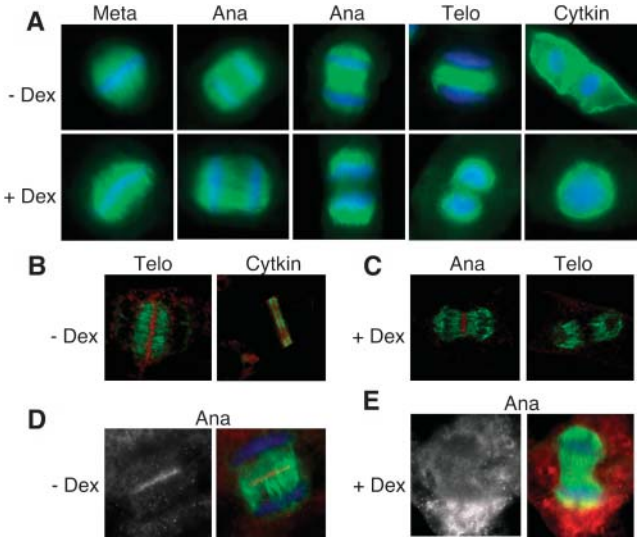

Figure 6. Immunodetection of MT Arrays, and KNOLLE and NACK1 Proteins in Noninduced and Dex-Induced CycBMut-GFP *N. tabacum* BY2 Cells.

(A) Immunostaining of α-tubulin (green) and staining of the chromatin with DAPI (blue) in noninduced cells (−Dex, top row) and in Dex-induced cells expressing the nondegradable cyclin (+Dex, bottom row). Representative cells in metaphase (Meta), anaphase (Ana), telophase (Telo), and cytokinesis (Cytkin) are shown.

(B) and **(C)** The syntaxin KNOLLE localizes to the midzone band during anaphase but disappears from this site in late telophase in CycBMut-GFP expressing cells. Double immunolabeling of tubulin (green) and KNOLLE (red) in noninduced cells **(B)** and in Dex-induced cells expressing CycBMut-GFP **(C)**. Representative cells in late anaphase (Ana) and telophase (Telo) are shown.

(D) and **(E)** The NACK1 protein localizes to the midzone band during anaphase in noninduced cells (−Dex) but not in Dex-induced cells expressing the nondegradable cyclin (+Dex). Immunostaining of the NACK1 protein shown at left, whereas merged images showing immunostaining of NACK1 (red) and α-tubulin (green) and staining of the chromatin with DAPI (blue) are shown at right.

midzone of abnormally long early anaphase spindle (Figure 6C, Ana), but it was not observed in cells in which the midzone anaphase MTs were completely disorganized or absent. Correspondingly, the KNOLLE signal was also completely lost from the midline of cells in which phragmoplast was not formed (Figure 6C, Telo). Together, these data indicate that the cells initiated a cell plate formation during anaphase, but at later stages it became destabilized and aborted, probably as a consequence of a failure to transform the anaphase midzone MT array into a phragmoplast.

Cytokinesis-specific kinesin NACK1 was only present on the midzone from anaphase to telophase in control cells (Figure 6D), decorating strongly the midline in the area of cell plate formation. Contrary to KNOLLE, when CycB1 expression was induced in the presence of Dex, NACK1 signal was never observed to accumulate in the midzone of cells with an aberrant anaphase spindle, but the labeling remained diffuse in the cytoplasm (Figure 6E). Thus, ectopic expression of nondegradable cyclin B1 during late mitosis interferes with localization of NACK1 to the midzone of anaphase spindle, which might contribute to altered MT dynamics, leading to impaired phragmoplast and cell plate formation.

DISCUSSION

Degradation of mitotic cyclins is a hallmark of the exit from mitosis in all eukaryotes. A prevailing idea is that this degradation leads to a drop of Cdc2 kinase activity that is required for spindle disassembly, chromosome decondensation, daughter nuclear envelope reformation, and cytokinesis. However, in animals, the cellular consequences of overexpressing nondegradable forms of cyclins are leading to a cell cycle delay or block whose timing depends on the class of cyclin used. Thus, in *D. melanogaster*, expression of stable forms of cyclin A, B, and B3 result in a metaphase delay, an early anaphase block, and a late anaphase block, respectively (Sigrist et al., 1995; Parry and O'Farrell, 2001). In plants, the posttranscriptional regulations and functions of mitotic cyclins are still extremely poorly understood. The increased number of cyclins compared with other higher eukaryotes adds even more complexity (Renaudin et al., 1996; Vandepoele et al., 2002). Furthermore, it is still not clear whether all mitotic cyclins have to be destroyed at the end of plant mitosis as is known for other eukaryotes (Mironov et al., 1999; Capron et al., 2003).

In this study, we investigated the consequences of strong nondegradable cyclin B1 expression, both in planta and in cell suspension culture. The transgenic plants exhibited different morphological phenotypes that were dependent on the level of ectopic cyclin expression. Plants expressing a moderate level of the transgene showed mainly asymmetric and blistered leaves, whereas at higher expression levels severe developmental defects were observed, leading to seedling postgermination death in the most extreme cases. Thus, strong expression of nondegradable cyclin B1 in plants, like in *D. melanogaster* (Rimmington et al., 1994), is lethal.

The nondegradable cyclin B1–overexpressing plants exhibited phenotypes similar to plants that overexpress negative regulators of the cell cycle. Thus, overexpression of different CKIs (or Kip-related proteins) produces in Arabidopsis serration and/or undulation of the leaves, as well as reduced plant growth and an increase in the cell size (Wang et al., 2000; De Veylder et al., 2001; Jasinski et al., 2002). An increase in the size of different cells has also been observed by overexpressing a dominant-negative, and, thus, an inactive version of CDK-A kinase in *N. tabacum* (Hemerly et al., 1995). It appears that increased cell size compensates for the lower cell number resulting from cell cycle arrest or other major cell cycle defects. By contrast, plants overexpressing positive regulators of the cell cycle, like cyclin D3 (Dewitte et al., 2003) or the E2Fa-DPa transcription factor (De Veylder et al., 2002), produce more cells with smaller size.

Interestingly, a mutation of the Arabidopsis *HOBBIT* gene that encodes a putative subunit of the ubiquitin protein ligase involved in cyclin B degradation, the APC/C (reviewed in Harper et al., 2002; Peters, 2002), has recently been reported (Blilou et al., 2002). This mutant was described previously to be

impaired in root meristem formation (Willemsen et al., 1998). However, a more detailed analysis of the mutant phenotype revealed multiple defects in maintenance of cell division and postembryonic progression of cell differentiation (Blilou et al., 2002). Although it has not yet been demonstrated that the HOBBIT protein is part of the plant APC/C complex, the *hobbit* mutants are expected to accumulate many mitotic cell cycle regulators, including the B-type cyclins.

Strikingly, several phenotypic similarities to the *hobbit* mutants, at least for the weak alleles, were observed in the strong nondegradable cyclin B1–overexpressing plants. Among them, undifferentiated cotyledons, radial swelling of the hypocotyls, irregular shape of epidermal leaf, and cotyledon cells and vacuolated cells that did not differentiate appropriately. However, we never observed a total absence of root or shoot meristematic activity, as is described in the strong *hobbit* alleles. Based on our observations, it is probable that the *hobbit* phenotypes could, at least in part, be attributed to the nondegradation of mitotic cyclins.

To identify the origin of the cell cycle defects produced by the nondegradable cyclin B1, we performed a detailed microscopic analysis of synchronized BY2 cells expressing the mutant protein under the control of an inducible promoter. The nondegradable cyclin B1 had no or only very limited effects on S-phase progression and on the G2-to-M transition. There were also no visible effects on the early events of mitosis until metaphase, the stage when cyclin B1 is normally degraded (Criqui et al., 2001). Thus, in plants, as reported for most eukaryotes, the inactivation of M phase–promoting factor is not required for the onset of anaphase. The only exception was found in mammalian cells, in which a low level of nondegradable cyclin B1 (less than 30% of the endogenous cyclin B1) was sufficient to block the metaphase–anaphase transition (Chang et al., 2003). Although sister chromatid separation did not require the degradation of the plant cyclin B1, mitotic abnormalities were detected during anaphase, with the gradual disappearance of the midzone MTs of the late anaphase spindle. This resulted in telophase-like cells with two separated nuclei with highly condensed chromatin but without phragmoplast and, hence, cytokinesis did not occur.

Surprisingly, in most cells we observed the fusion of the daughter nuclei in a process similar to endomitosis (reviewed in Edgar and Orr-Weaver, 2001; see below). Whether certain resulting pseudo-G1 polyploid cells still have the capacity to divide a second time is unknown. Flow cytometric analyses and microscopic characterization of the strong nondegradable cyclin B1–overexpressing plants indicated that this phenomenon also occurred in planta. Fusion of the daughter nuclei has never been reported in fungi or animal cells overproducing mitotic cyclins. The overexpression of the Aurora-A kinase in human cells produces an aberrant cytokinesis, giving rise to multinucleated cells, the nuclei of which did not fuse (Meraldi et al., 2002). Nevertheless, endomitosis has been reported to occur in animal cells. Thus, mammalian megakaryocytes blood cells become highly polyploid by endomitosis. In these cells, the chromosomes condense, the nuclear envelop breaks down, and sister chromatids separate in anaphase A, but anaphase B does not occur. At a stage equivalent to telophase, the chromosomes are incorporated into the same nucleus. Although the mechanism(s) leading to the abortive mitosis is unknown, the possibility that cyclin B1/CDK1 is involved in this process has been hypothesized (Vitrat et al., 1998; Carow et al., 2001).

Based on our observations, it is clear that the major consequence of maintaining a high level of cyclin B1 after metaphase is an alteration of MT organization and dynamics, which is leading to impaired formation of a phragmoplast. MT dynamics are regulated by different proteins, including MT stabilizing and destabilizing factors, as well as MT nucleators (Desai and Mitchison, 1997). During mitosis MTs are in a state of higher dynamics instability, which is changed to a more stable state by the end of mitosis (Manabe et al., 2002). After Cdc2 kinase downregulation, spindle assembly factors are dephosphorylated, which leads to changes in MT dynamics and spindle disassembly. MT-associated proteins are targets of animal cyclin B1/CDK1 complex (Vasquez et al., 1999). In plants, different MT-associated proteins have also been characterized, and some of them seem to play an essential role in the stability of certain MT arrays (reviewed in Lloyd and Hussey, 2001). However, there is only little evidence that cyclin/CDK activity controls MT dynamics in plants. Microinjection in stamen hair cells of affinity purified active mitotic CDK complexes accelerated prophase progression and produced a rapid destabilization of the PPB (Huch et al., 1996), whereas roscovitine, a specific CDK inhibitor, led to abnormal mitotic spindle formation (Binarova et al., 1998).

Thus, the overexpression of nondegradable cyclin B1 and, as a consequence, a high CDK activity during late mitosis may keep MTs in a mitotic dynamic status preventing their rearrangement into anaphase and telophase arrays. The dominant assembly of MTs around clusters of highly condensed separated sister chromatids, as well as in vicinity of pseudo-G1 nuclei in endomitotic cells, might be a result of the stabilizing effect of chromatin on mitotic MTs. Chromatin is known to positively influence MT stability via local signaling gradients, which can determine centrosome position, MT length, and spindle size and organization by influencing motor activities, chromatin-mediated phosphorylation, and the small GTPase Ran machinery (Karsenti and Vernos, 2001). A long-range guidance effect of chromatin on MT dynamics during spindle organization has also recently been demonstrated (Carazo-Salas and Karsenti, 2003).

During plant cytokinesis, the phragmoplast forms a cytoskeletal structure consisting of two antiparallel bundles of MTs, which have plus ends overlapping in the midzone. This structure serves as a scaffold along which Golgi-derived vesicles, carrying cell plate material, are transported to the equatorial plane, where the fusion of these vesicles initiates the formation of a cell plate (reviewed in Smith, 2002). A number of proteins related to vesicle trafficking, as well as MT-associated proteins, kinesin-like motor proteins, and several protein kinases, are involved in this process and specifically localized to the phragmoplast or its midzone (Nishihama et al., 2001). Among them is NACK1, a *N. tabacum* kinesin-like protein, which associates with and regulates the activity of NPK1, a *N. tabacum* MAP kinase kinase kinase. Both proteins are localized to the equatorial region of the phragmoplast MTs and are essential for the outgrowth of the phragmoplast, which involves MT depolymerization at the inside and repolymerization at the outside toward the parental wall

(Nishihama et al., 2002). We found that the localization of NACK1 to the equatorial line was disrupted in cells expressing nondegradable cyclin B1, and short interdigitated phragmoplast MTs could not be formed. Downregulation of NACK1 by viral-induced gene silencing (Nishihama et al., 2002) or mutation in its Arabidopsis homolog, HINKEL (Strompen et al., 2002), allows the formation of a phragmoplast, but either its expansion or stability is altered. The failure to organize a phragmoplast when cyclin B1 persists into anaphase might be because of overstabilized MTs already at anaphase, which often persisted and interconnected even the decondensing nuclei. However, at later stages the long interconnected anaphase MTs fall apart. This could account for the failure of NACK1 to transport regulators that are important for the stabilization of MTs at the midline. Interestingly, we found that NtMAP65-1 (Smertenko et al., 2000) was associated with anaphase MTs in cells expressing nondestructible cyclin B1, but its accumulation at the midline was prevented (Weingartner, unpublished results). NtMAP65-1 is known to cross-bridge MTs (Lloyd and Hussey, 2001) and thus might be important for organizing phragmoplast MTs. The inability of MAP65-1 to move to the midline could result in the inappropriate overstability of anaphase MTs, whereas its lack at the midline and consequently its failure to cross-bridge MTs there might cause these abnormal spindles to fall apart. MAP65-1 proteins also have predicted phosphorylation sites both for CDK and MAP kinases (Nishihama et al., 2001; Jonak et al., 2002).

NPK1 was shown to be activated specifically during late stages of mitosis, and its activity was regulated by changing the degree of its own phosphorylation with the hyperphosphorylated form of NPK1 showing very low activity (Nishihama et al., 2001). CDKs might be candidate kinases for keeping NPK1 inactive during early mitosis because NPK1 has possible CDK phosphorylation sites (Jonak et al., 2002). Whether the phosphorylation of NPK1 is changed upon ectopic cyclin B expression during late mitosis remains to be determined. By contrast, the subcellular localization of the syntaxin homolog KNOLLE to the midplane of late anaphase spindles was not disturbed even in cells with abnormal spindles, suggesting that the transport of vesicles along MTs was not impaired in these cells. This is consistent with the results of KNOLLE localization in the *hinkel* mutant, which is also not affected (Strompen et al., 2002).

In animal cells, it has been shown that cyclin B1 associates with CDK1 to fulfill its mitotic functions. In contrast with animals, higher plants seem also to require for the G2-to-M transition a more divergent class of CDKs (called the B-type) that do not contain the characteristic PSTAIRE motif (Porceddu et al., 2001). Until now, the identity of the CDK partner(s) of cyclin B1 was unknown. Here, we show that plant cyclin B1 is able to bind and activate both A- and B-type CDKs. Subcellular localization experiments performed with cyclin B1-GFP fusions demonstrated that the proteins mainly associate with condensing chromatin and remain on the chromosomes until metaphase, when they become destroyed (Criqui et al., 2001). An A-type CDK from alfalfa also binds transiently to the chromosomes at the metaphase–anaphase transition (Stals et al., 1997). Furthermore, visualization of the GFP-tagged CDK Medsa;CDK;A;2 in living *N. tabacum* cells revealed that the kinase associates strongly to condensing chromosomes but leaves the chromatin before prometaphase (Weingartner et al., 2001). Thus, B1-type cyclins may well interact with A-type CDKs to eventually trigger chromosome condensation and nuclear envelope breakdown, but at later stages the chromatin-associated cyclin B1 must have another partner because the nondegradable cyclin B1 remained associated with the nuclear material throughout anaphase and telophase (Criqui et al., 2001; this study), whereas the GFP-tagged A-type CDK was found along the mitotic spindle and subsequently the phragmoplast (Weingartner et al., 2001). In contrast with the A-type CDKs, a tight association with the two sets of chromosomes during anaphase has been described for a B-type CDK from rice (Lee et al., 2003). Therefore, it is possible that the nondegradable cyclin B1 associates with a B-type CDK during anaphase.

Higher plant cells lack a defined and structured MT-organizing center, such as the centrosome in animal cells and the spindle pole body in *S. cerevisiae* (Schmit, 2002). Mazia (1984) proposed that plant cells have a flexible centrosome, in which the MT-nucleating material is free to assume various locations during the cell cycle. However, a centrosome-independent, MT-nucleation pathway is also important in cells equipped with centrosomes and occurs both in cytoplasm and in association with chromatin (Maly and Borisy, 2002). Interestingly, we found in the pseudo-G1 cells an abnormal organization of the cortical MTs. It is well known that cortical MTs disappear from the cell cortex at M phase but become reorganized during G1 phase to regulate the direction of cell elongation. Recently, several data provide new insights into the mechanisms controlling cortical MT assembly and dynamics. Observation of individual MTs revealed that they are initiated at the cell cortex and exhibit dynamics at both ends (Shaw et al., 2003). Moreover, it has been proposed that cortical MTs initially originate at the daughter nuclear surface after mitosis and that further reorganization occurs on the cell cortex (Kumagai et al., 2003, and references therein). Homologs of proteins implicated in nucleation and dynamics of spindle MTs in animal cells, such as TOG, XMAP215, and katanin p60 were also found to act on cortical MTs in plants (Wasteneys, 2002). The Arabidopsis *mor1* mutant, which is an XMAP 215 homolog (Whittington et al., 2001), is specifically impaired in the organization of the cortical MTs and shows isotropic cell expansion similar to our transgenic plants. The strong nondegradable cyclin B1–overexpressing plants exhibited cells in different tissues with an extremely abnormal shape and a reduction and/or disorientation of cortical MTs. How nondegradable cyclin B1 affects cortical MT organization in our transgenic plants is unknown. Nevertheless, it is noteworthy that in *S. cerevisiae*, mitotic cyclin CLB1 or CLB2-mediated activity depolarizes the cytoskeleton and thereby permits isotropic bud growth and, thus, control cell morphogenesis (Lew and Reed, 1993).

METHODS

Chemicals

Propyzamide was obtained from Sumitomo Chemical (Osaka, Japan). Dexamethasone (Sigma-Aldrich, St. Louis, MO) was dissolved in ethanol and kept at a concentration of 30 mM.

Cyclin Constructs

We used PCR-based, site-directed mutagenesis to introduce an epitope of an 11 amino acid peptide (EQKLISEEDLN) from the human *c-myc* gene at the C terminus of the *N. tabacum* cyclin B1 (Nicta;CycB1;1), as well as the BamHI and SacI cloning sites. The PCR reaction was performed using oligonucleotide 1 (5′-CAAGAAGGATCCCTTCAAATGGATAAC-3′) and oligonucleotide 2 (5′-GCAGTAAAAGAGCTCTCAATTAAGGTCCTCTTC-AGAGATGAGTTTCTGTTCAGAAGAGGAGGAAGCAGCATC-3′) as the upstream and downstream primers, respectively. The BamHI-SacI fragment was cloned into pBluescript SKII+ (Stratagene, La Jolla, CA) vector, resulting in pSKCycB*myc*. pSKmutD-boxCycB*myc* differs from pSKCycB*myc* by mutation of two highly conserved amino acids of the D-box motifs from RxxLxxIxN to GxxVxxIxN using oligonucleotide 3 (5′-AAGAAATGGACGTGCTGTTGGAGAC-3′) and oligonucleotide 4 (5′-CCATCGGCTTGTGCATTTTTCTG-3′) as PCR primers. Both constructs were sequenced on both strands to confirm their sequences. The BamHI-SacI DNA fragments from each construct (pSKCycB*myc* and pSKmutD-boxCycB*myc*) were subcloned into the binary pBI121.1 vector (CLONTECH, Palo Alto, CA) by replacing the *GUS* reporter gene, resulting in pBICycB*myc* and pBImutD-boxCycB*myc*, respectively. The GFP-tagged cyclin constructs are described in Criqui et al. (2000).

Plant Transformation and Regeneration

Seeds of *N. tabacum* var Samsun NN were surface-sterilized by treatment with 5% sodium hypochloride for 15 min, then rinsed six times with sterile water and germinated on a 0.8% agar medium containing Murashige and Skoog (MS) salts (Duchefa, Haarlem, The Netherlands) and 1% sucrose. The plants were grown either in vitro in a 22°C growth chamber or in a greenhouse under a 12-h-light/12-h-dark cycle at 18 to 25°C.

The protocol used for plant transformation and regeneration was first described by Horsch et al. (1985) and then modified by Atanassova et al. (1995). To induce callus formation, leaf strips were incubated in MS medium containing 30 g/L of sucrose, 2 mg/L of 6-benzylaminopurine (Serva, Heidelberg, Germany), and 0.05 mg/L of naphthaleneacetic acid (Serva). The plantlets were cultured in vitro until they grew sufficient roots and then transferred to the greenhouse. Seeds obtained from T0 plants by self-pollination were germinated on MS medium supplemented with 100 mg/L kanamycin to get transformed T1 plants.

Histological Analysis and Immunofluorescence Labeling of *N. tabacum* Seedlings

Pictures from 20 d–postgermination seedlings were taken with a stereomicroscope (Leica MZ12; Wetzlar, Germany). For environmental scanning electron microscopy, 9 d–postgermination seedlings were directly visualized on a Philips XL30 environmental scanning electron microscope (Eindhoven, The Netherlands).

For histological analysis, seedlings were sampled 20 d postgermination. Plant material was fixed in 100 mM phosphate buffer, pH 7.2, containing 1% glutaraldehyde, and postfixed at room temperature in 100 mM phosphate buffer, pH 7.2, containing 0.1% OsO_4 and embedded in LR White resin (EMS, Fort Washington, PA) or Paraplast X-TRA (EMS). Respectively, 0.5- and 10-μm sections were prepared and stained with 1% (w/v) toluidine blue for morphological analysis. Images were taken on a Nikon TE 2000 microscope (Tokyo, Japan) with a Sony DXMI200 camera (Tokyo, Japan).

For immunostaining, seedlings were sampled 8 d postgermination. Plant material was fixed for 40 min with 1.5% paraformaldehyde and 0.5% glutaraldehyde in MT-stabilizing buffer (100 mM Pipes, 4 mM EGTA, and 4 mM $MgSO_4$, pH 7.2) containing 0.05% Triton X-100, postfixed for 10 min in cold methanol, and washed in PBS buffer. Samples were then transferred to freshly prepared PBS containing 0.1% (w/v) $NaBH_4$ for 20 min to reduce autofluorescence before a 15-min treatment with 0.2% (w/v) pectolyase Y23 (Seishin, Tokyo, Japan), 1% (w/v) macerozyme R10 (Serva), and 3% (w/v) caylase 345 (CAYLA, Toulouse, France) in digestion buffer (600 mM mannitol, 8 mM $CaCl_2$, and 25 mM Mes, pH 5.5) to partially digest cell walls. After three washes in PBS containing 50 mM Gly and 0.05% Triton X-100, seedlings without the aerial parts were gently squashed between two poly-L-Lys–coated coverslips before the addition of blocking solution consisting of PBS, 5% (w/v) BSA, and 5% (v/v) normal goat serum for 20 min at room temperature. MT staining was performed using an anti-α-tubulin mouse monoclonal antibody (Amersham, Buckinghamshire, UK) at a dilution of 1:5000, followed by secondary antibody Alexa-fluor 488 goat anti-mouse IgG (Molecular Probes Europe, Leiden, The Netherlands) diluted 1:100. Confocal laser microscopy was performed using a Zeiss LSM510 laser-scanning confocal microscope (Jena, Germany).

Synchronization of BY2 Cells and Cell Cycle Analysis

Synchronization was performed by diluting a 7-d-old culture 1:5 and adding 10 mg/L aphidicolin (Sigma) 8 h later for 16 h. After removal of the aphidicolin by washing cells five times with medium, the cells were incubated in fresh medium with 0.5 μM Dex to induce cyclin B1-GFP expression. To block cells in prometaphase, 10 μM propyzamide was added 7 h after aphidicolin release and after 6-h incubation removed by washing five times with fresh medium. For mitotic index, cells were fixed in a 3:1 (v/v) ethanol:acetic acid mixture, then washed with 70% (v/v) ethanol. The DNA was stained with 1 μg/mL DAPI and observed by epifluorescence microscopy.

Immunostaining and Microscopy of the BY2 Cells

For indirect immunofluorescence, cells were fixed and stained as described previously (Bögre et al., 1997). MT staining was performed using an anti-α-tubulin mouse monoclonal antibody, DM1A (Sigma), at a dilution of 1:200 and anti-mouse fluorescein isothiocyanate–conjugated secondary antibody (Sigma). DNA was stained with 1 μg/mL DAPI in PBS. For KNOLLE staining, an anti-KNOLLE rabbit polyclonal antibody (Rose Biotech, Winchendon, MA) at a dilution of 1:2000 and goat anti-rabbit Alexa-fluor 568 secondary antibody (Molecular Probes Europe) at a dilution of 1:300 were used. For NACK1 staining, anti-NACK1 rabbit polyclonal antibody at a dilution of 1:10 and anti-rabbit cy3-conjugated secondary antibody (Sigma) at a 1:100 dilution were used.

For GFP observation, a drop of cell suspension was transferred on a slide, carefully covered with a coverslip, and observed with an upright fluorescence microscope (Axioplan 2; Zeiss) equipped with a GFP filter (HQ480/20X and HQ510/20M; AF Analysentechnik, Jena, Germany). Typical exposure times were in a range of few seconds. Images were taken using a cooled charge-coupled device black-and-white digital camera (SPOT-2; Diagnostic Instruments, Burroughs, MI) and Metaview imaging software (Diagnostic Instruments). Confocal images were taken by a Zeiss laser-scanning confocal microscope with argon laser excitation at 488 nm and through 505 to 550 nm emission filter set using a C-APOCHROMAT (40×) oil objective lens.

RNA Gel Blotting and RT-PCR Analysis

RNA was extracted from leaves using the Trizol reagent (Invitrogen, Carlsbad, CA). RNA gels were performed with 20 μg of total RNA per lane. The RNA gel blotting procedure is described in Genschik et al. (1998). The cyclin B1;1 probe corresponds to the Nicta;CycB1;1 cDNA (Qin et al., 1996). Ethidium bromide staining and hybridization with a probe encoding the translation elongation factor-1α (EF-1α) (At1g07920) verified the integrity and the amount of RNA applied to each lane.

For RT-PCR, 2 μg of total RNA (treated with the DNase A) (Qiagen USA, Valencia, CA) was used for first-strand cDNA synthesis using the Superscript RT II kit (Gibco BRL) and oligo(dT) (Eurogentec, Herstal, Belgium) according to manufacturer's instructions. One-microliter aliquot of the RT reaction (20 μL) was used as a template in the RT-PCR amplification reactions. After 30 PCR amplification cycles, 15 μL from the reaction was separated on a 1.5% agarose gel. The primers used to detect cyclin B1 gene expression were: OL-D-box (5′-GGAAGAAA-TAGGCGTGCTCTC-3′), OL-Δ(D-box) (5′-GGAAGAAATGGACGTGCT-GTT-3′), OL-1 (5′-CTTGGCTGGTACATCTTTATTGAC-3′), OL-2 (5′-AGTCCACAAGCAGCCTTGC-3′), OL-3 (5′-AAGCTGCAACACCATCTG-ATAAT-3′), and OL-myc (5′-AAGGTCCTCTTCAGAGATGAGTTTC-3′). The primer set used to detect *actin* gene expression was OL-act1 (5′-GATATGGAGAARATMTGGCATCAYAC-3′) and OL-act2 (5′-GTT-TCRTGAATWCCWGCWGCTTCCATTCC-3′).

In Vitro Protein Interaction

Arath;CYCB1;1 was N-terminally His-tagged and inserted in pEU3-NII vector. Arath CDKA;1 and CDKB2;1 were subcloned into the same vector without tag. In vitro transcription and translation were conducted in wheat germ extract according to Proteios kit batch translation protocol (Invitrotech, Kyoto, Japan). Completing the translation reaction, the volume of the mixtures was adjusted 250 μL with PBS and overnight dialyzed against PBS at 4°C. Fifty microliters of translation samples were mixed as indicated and coupled to 10 μL Ni-agarose (Qiagen USA) for 2 h at 4°C. The beads were washed with excess washing buffer (50 mM NaH_2PO_4, 300 mM NaCl, and 30 mM imidazole) and analyzed on immunoblot and in kinase assay.

Polyclonal Arath;CDKA;1 and Arath;CDKB2;1 antibodies were raised against the peptides derived from the C termini of the respective proteins (courtesy of L. Bakó). SDS-PAGE and protein gel blots were performed according to standard procedures, with primary antibodies diluted 1:1000 and a secondary peroxidase-conjugated antibody (Amersham Pharmacia Biotech, Uppsala, Sweden) diluted 1:10000. His-tagged cycB1;1 was detected by monoclonal anti-polyhistidine peroxidase conjugate (Sigma) following the manufacturer's protocol. The blots were incubated in SuperSignal West Pico (Pierce, Rockford, IL) and exposed. The kinase reaction has been described previously (Magyar et al., 1997).

Immunoprecipitation, $p9^{CksHs1}$ Binding, and Histone H1 Kinase Assay

Total protein extracts were prepared as described previously (Weingartner et al., 2001). CDK activities were measured after immunoprecipitation with polyclonal rabbit antisera raised against NtCdkA (kindly provided by Masami Sekine, Nara, Japan) or after binding to $p9^{CksHs1}$ beads. Washing conditions of the beads and the histone H1 kinase reactions were performed as described previously (Bögre et al., 1997).

ACKNOWLEDGMENTS

We thank Tobacco Science Research Laboratory, Japan Tobacco, for allowing us to use the TBY2 cell suspension, the ABRC for providing the EF-1α (cDNA clone 232A19T7), Masami Sekine for NtCdkA antibody, Yasunori Machida for the NACK1 antibody, Dirk Inzé for the $p9^{CksHs1}$ beads, l'Université Louis Pasteur de Strasbourg, Centre National de la Recherche Scientifique, L'Association pour la Recherche sur le Cancer, La Ligue Nationale Contre le Cancer and Région Alsace for founding the confocal microscope, and Philippe Hammann for DNA sequencing. We also thank Erwin Heberle-Bors (Vienna Biocenter, Vienna, Austria) for his generous help and support, especially during the initial phase of this project. M.W. was supported by Action Concertée Incitative Jeune Chercheur from the French Ministry of Research and by European Union Framework 5 Grant HPRN-CT-2002-00333. T.M. was supported by a Marie Curie fellowship. The work in the lab of L.B. was supported by Biotechnology and Biological Sciences Research Council Grant P13340 and by collaborative Wellcome Trust Grant 06741/Z/02/Z to L.B. and P.B.

Received December 16, 2003; accepted January 5, 2004.

REFERENCES

Amon, A., Irniger, S., and Nasmyth, K. (1994). Closing the cell cycle circle in yeast: G2 cyclin proteolysis initiated at mitosis persists until the activation of G1 cyclins in the next cycle. Cell **77,** 1037–1050.

Aoyama, T., and Chua, N.H. (1997). A glucocorticoid-mediated transcriptional induction system in transgenic plants. Plant J. **11,** 605–612.

Atanassova, R., Favet, N., Martz, F., Chabbert, B., Tollier, M.T., Monties, B., Fritig, B., and Legrand, M. (1995). Altered lignin composition in transgenic tobacco expressing O-methyltransferase sequences in sense and antisense orientation. Plant J. **8,** 465–477.

Azimzadeh, J., Traas, J., and Pastuglia, M. (2001). Molecular aspects of microtubule dynamics in plants. Curr. Opin. Plant Biol. **4,** 513–519.

Binarova, P., Dolezel, J., Draber, P., Heberle-Bors, E., Strnad, M., and Bogre, L. (1998). Treatment of *Vicia faba* root tip cells with specific inhibitors to cyclin-dependent kinases leads to abnormal spindle formation. Plant J. **16,** 697–707.

Blilou, I., Frugier, F., Folmer, S., Serralbo, O., Willemsen, V., Wolkenfelt, H., Eloy, N.B., Ferreira, P.C., Weisbeek, P., and Scheres, B. (2002). The *Arabidopsis* HOBBIT gene encodes a CDC27 homolog that links the plant cell cycle to progression of cell differentiation. Genes Dev. **16,** 2566–2575.

Bögre, L., Zwerger, K., Meskiene, I., Binarova, P., Csizmadia, V., Planck, C., Wagner, E., Hirt, H., and Heberle-Bors, E. (1997). The cdc2Ms kinase is differently regulated in the cytoplasm and in the nucleus. Plant Physiol. **113,** 841–852.

Capron, A., Okresz, L., and Genschik, P. (2003). First glance at the plant APC/C, a highly conserved ubiquitin-protein ligase. Trends Plant Sci. **8,** 83–89.

Carazo-Salas, R.E., and Karsenti, E. (2003). Long-range communication between chromatin and microtubules in Xenopus egg extracts. Curr. Biol. **13,** 1728–1733.

Carow, C.E., Fox, N.E., and Kaushansky, K. (2001). Kinetics of endomitosis in primary murine megakaryocytes. J. Cell. Physiol. **188,** 291–303.

Chang, D.C., Xu, N., and Luo, K.Q. (2003). Degradation of cyclin B is required for the onset of anaphase in Mammalian cells. J. Biol. Chem. **278,** 37865–37873.

Criqui, M.C., and Genschik, P. (2002). Mitosis in plants: How far we have come at the molecular level? Curr. Opin. Plant Biol. **5,** 487–493.

Criqui, M.C., Parmentier, Y., Derevier, A., Shen, W.H., Dong, A., and Genschik, P. (2000). Cell cycle-dependent proteolysis and ectopic overexpression of cyclin B1 in tobacco BY2 cells. Plant J. **24,** 763–773.

Criqui, M.C., Weingartner, M., Capron, A., Parmentier, Y., Shen, W.H., Heberle-Bors, E., Bogre, L., and Genschik, P. (2001). Subcellular localisation of GFP-tagged tobacco mitotic cyclins during the cell cycle and after spindle checkpoint activation. Plant J. **28,** 569–581.

Cross, F.R., Yuste-Rojas, M., Gray, S., and Jacobson, M.D. (1999). Specialization and targeting of B-type cyclins. Mol. Cell **4,** 11–19.

Desai, A., and Mitchison, T.J. (1997). Microtubule polymerization dynamics. Annu. Rev. Cell Dev. Biol. **13,** 83–117.

De Veylder, L., Beeckman, T., Beemster, G.T., de Almeida Engler,, J., Ormenese, S., Maes, S., Naudts, M., Van Der Schueren, E., Jacqmard, A., Engler, G., and Inze, D. (2002). Control of proliferation, endoreduplication and differentiation by the *Arabidopsis* E2Fa-DPa transcription factor. EMBO J. **21,** 1360–1368.

De Veylder, L., Beeckman, T., Beemster, G.T., Krols, L., Terras, F., Landrieu, I., van der Schueren, E., Maes, S., Naudts, M., and Inze, D. (2001). Functional analysis of cyclin-dependent kinase inhibitors of *Arabidopsis*. Plant Cell **13,** 1653–1668.

Dewitte, W., Riou-Khamlichi, C., Scofield, S., Healy, J.M., Jacqmard, A., Kilby, N.J., and Murray, J.A. (2003). Altered cell cycle distribution, hyperplasia, and inhibited differentiation in *Arabidopsis* caused by the D-type cyclin CYCD3. Plant Cell **15,** 79–92.

Edgar, B.A., and Orr-Weaver, T.L. (2001). Endoreplication cell cycles: More for less. Cell **105,** 297–306.

Foley, E., and Sprenger, F. (2001). The cyclin-dependent kinase inhibitor Roughex is involved in mitotic exit in *Drosophila*. Curr. Biol. **11,** 151–160.

Gallant, P., and Nigg, E.A. (1992). Cyclin B2 undergoes cell cycle-dependent nuclear translocation and, when expressed as a non-destructible mutant, causes mitotic arrest in HeLa cells. J. Cell Biol. **117,** 213–224.

Gallant, P., and Nigg, E.A. (1994). Identification of a novel vertebrate cyclin: Cyclin B3 shares properties with both A- and B-type cyclins. EMBO J. **13,** 595–605.

Genschik, P., Criqui, M.C., Parmentier, Y., Derevier, A., and Fleck, J. (1998). Cell cycle-dependent proteolysis in plants: Identification of the destruction box pathway and metaphase arrest produced by the proteasome inhibitor MG132. Plant Cell **10,** 2063–2076.

Glotzer, M., Murray, A.W., and Kirschner, M.W. (1991). Cyclin is degraded by the ubiquitin pathway. Nature **349,** 132–138.

Harper, J.W., Burton, J.L., and Solomon, M.J. (2002). The anaphase-promoting complex: It's not just for mitosis any more. Genes Dev. **16,** 2179–2206.

Hemerly, A., Engler Jde, A., Bergounioux, C., Van Montagu, M., Engler, G., Inze, D., and Ferreira, P. (1995). Dominant negative mutants of the Cdc2 kinase uncouple cell division from iterative plant development. EMBO J. **14,** 3925–3936.

Holloway, S.L., Glotzer, M., King, R.W., and Murray, A.W. (1993). Anaphase is initiated by proteolysis rather than by the inactivation of maturation-promoting factor. Cell **73,** 1393–1402.

Horsch, R.B., Fry, J.E., Hoffmann, N.L., Eichholtz, D., Rogers, S.G., and Fraley, R.T. (1985). A simple and general method for transferring genes into plants. Science **227,** 1229–1231.

Huch, J., Wu, L., John, P.C.L., Hepler, L.H., and Hepler, P.K. (1996). Plant mitosis promoting factor disassembles the microtubule preprophase band and accelerates prophase progression in *Tradescantia*. Cell Biol. Int. **20,** 275–287.

Irniger, S. (2002). Cyclin destruction in mitosis: A crucial task of Cdc20. FEBS Lett. **532,** 7–11.

Jackman, M., Lindon, C., Nigg, E.A., and Pines, J. (2003). Active cyclin B1-Cdk1 first appears on centrosomes in prophase. Natl. Cell Biol. **5,** 143–148.

Jasinski, S., Riou-Khamlichi, C., Roche, O., Perennes, C., Bergounioux, C., and Glab, N. (2002). The CDK inhibitor NtKIS1a is involved in plant development, endoreduplication and restores normal development of cyclin D3; 1-overexpressing plants. J. Cell Sci. **115,** 973–982.

Jonak, C., Okresz, L., Bogre, L., and Hirt, H. (2002). Complexity, cross talk and integration of plant MAP kinase signalling. Curr. Opin. Plant Biol. **5,** 415–424.

Karsenti, E., and Vernos, I. (2001). The mitotic spindle: A self-made machine. Science **294,** 543–547.

Kimura, K., Hirano, M., Kobayashi, R., and Hirano, T. (1998). Phosphorylation and activation of 13S condensin by Cdc2 *in vitro*. Science **282,** 487–490.

Kreutzer, M.A., Richards, J.P., De Silva-Udawatta, M.N., Temenak, J.J., Knoblich, J.A., Lehner, C.F., and Bennett, K.L. (1995). *Caenorhabditis elegans* cyclin A- and B-type genes: A cyclin A multigene family, an ancestral cyclin B3 and differential germline expression. J. Cell Sci. **108,** 2415–2424.

Kumagai, F., Nagata, T., Yahara, N., Moriyama, Y., Horio, T., Naoi, K., Hashimoto, T., Murata, T., and Hasezawa, S. (2003). Gamma-tubulin distribution during cortical microtubule reorganization at the M/G1 interface in tobacco BY-2 cells. Eur. J. Cell Biol. **82,** 43–51.

Lauber, M.H., Waizenegger, I., Steinmann, T., Schwarz, H., Mayer, U., Hwang, I., Lukowitz, W., and Jurgens, G. (1997). The *Arabidopsis* KNOLLE protein is a cytokinesis-specific syntaxin. J. Cell Biol. **139,** 1485–1493.

Lee, J., Das, A., Yamaguchi, M., Hashimoto, J., Tsutsumi, N., Uchimiya, H., and Umeda, M. (2003). Cell cycle function of a rice B2-type cyclin interacting with a B-type cyclin-dependent kinase. Plant J. **34,** 417–425.

Lew, D.J., and Reed, S.I. (1993). Morphogenesis in the yeast cell cycle: Regulation by Cdc28 and cyclins. J. Cell Biol. **120,** 1305–1320.

Li, J., Meyer, A.N., and Donoghue, D.J. (1997). Nuclear localization of cyclin B1 mediates its biological activity and is regulated by phosphorylation. Proc. Natl. Acad. Sci. USA **94,** 502–507.

Lloyd, C., and Hussey, P. (2001). Microtubule-associated proteins in plants: Why we need a MAP. Natl. Rev. Mol. Cell Biol. **2,** 40–47.

Magyar, Z., Meszaros, T., Miskolczi, P., Deak, M., Feher, A., Brown, S., Kondorosi, E., Athanasiadis, A., Pongor, S., Bilgin, M., Bako, L., Koncz, C., and Dudits, D. (1997). Cell cycle phase specificity of putative cyclin-dependent kinase variants in synchronized alfalfa cells. Plant Cell **9,** 223–235.

Maly, I.V., and Borisy, G.G. (2002). Self-organization of treadmilling microtubules into a polar array. Trends Cell Biol. **12,** 462–465.

Manabe, R., Whitmore, L., Wiess, J.M., and Horwitz, A.R. (2002). Identification of a novel microtubule-associated protein that regulates microtubule organization and cytokinesis by using GFP-screening strategy. Curr. Biol. **12,** 1946–1951.

Mazia, D. (1984). Centrosomes and mitotic poles. Exp. Cell Res. **153,** 1–15.

Meraldi, P., Honda, R., and Nigg, E.A. (2002). Aurora-A overexpression reveals tetraploidization as a major route to centrosome amplification in p53−/− cells. EMBO J. **21,** 483–492.

Mews, M., Sek, F.J., Moore, R., Volkmann, D., Gunning, B.E.S., and John, P.C.L. (1997). Mitotic cyclin distribution during maize cell division: Implications for the sequence diversity and function of cyclins in plants. Protoplasma **200,** 128–145.

Minshull, J., Blow, J.J., and Hunt, T. (1989). Translation of cyclin mRNA is necessary for extracts of activated *Xenopus* eggs to enter mitosis. Cell **56,** 947–956.

Mironov, V., De Veylder, L., Van Montagu, M., and Inzé, D. (1999). Cyclin-dependent kinases and cell division in plants — The nexus. Plant Cell **11,** 509–522.

Murray, A.W., Solomon, M.J., and Kirschner, M.W. (1989). The role of cyclin synthesis and degradation in the control of maturation promoting factor activity. Nature **339,** 280–286.

Nagata, T., Nemoto, Y., and Hasezawa, S. (1992). Tobacco BY-2 cell line as the ''HeLa'' cell in the cell biology of higher plants. Int. Rev. Cytol. **132,** 1–30.

Nigg, E.A. (2001). Mitotic kinases as regulators of cell division and its checkpoints. Natl. Rev. Mol. Cell Biol. **2,** 21–32.

Nishihama, R., Ishikawa, M., Araki, S., Soyano, T., Asada, T., and Machida, Y. (2001). The NPK1 mitogen-activated protein kinase kinase kinase is a regulator of cell-plate formation in plant cytokinesis. Genes Dev. **15,** 352–363.

Nishihama, R., Soyano, T., Ishikawa, M., Araki, S., Tanaka, H., Asada, T., Irie, K., Ito, M., Terada, M., Banno, H., Yamazaki, Y., and Machida, Y. (2002). Expansion of the cell plate in plant cytokinesis requires a kinesin-like protein/MAPKKK complex. Cell **109,** 87–99.

Parry, D.H., and O'Farrell, P.H. (2001). The schedule of destruction of three mitotic cyclins can dictate the timing of events during exit from mitosis. Curr. Biol. **11,** 671–683.

Peters, J.M. (2002). The anaphase-promoting complex: Proteolysis in mitosis and beyond. Mol. Cell **9,** 931–943.

Pines, J. (1999). Four-dimensional control of the cell cycle. Natl. Cell Biol. **1,** 73–79.

Pines, J., and Hunter, T. (1989). Isolation of a human cyclin cDNA: Evidence for cyclin mRNA and protein regulation in the cell cycle and for interaction with $p34^{cdc2}$. Cell **58,** 833–846.

Pines, J., and Rieder, C.L. (2001). Re-staging mitosis: A contemporary view of mitotic progression. Natl. Cell Biol. **3,** E3–E6.

Porceddu, A., Stals, H., Reichheld, J.P., Segers, G., De Veylder, L., Barroco, R.P., Casteels, P., Van Montagu, M., Inze, D., and Mironov, V. (2001). A plant-specific cyclin-dependent kinase is involved in the control of G2/M progression in plants. J. Biol. Chem. **276,** 36354–36360.

Qin, L.X., Perennes, C., Richard, L., Bouvier-Durand, M., Trehin, C., Inze, D., and Bergounioux, C. (1996). G2- and early-M-specific expression of the NTCYC1 cyclin gene in *Nicotiana tabacum* cells. Plant Mol. Biol. **32,** 1093–1101.

Renaudin, J.P., et al. (1996). Plant cyclins: A unified nomenclature for plant A-, B- and D-type cyclins based on sequence organization. Plant Mol. Biol. **32,** 1003–1018.

Rimmington, G., Dalby, B., and Glover, D.M. (1994). Expression of N-terminally truncated cyclin B in the *Drosophila* larval brain leads to mitotic delay at late anaphase. J. Cell Sci. **107,** 2729–2738.

Schmit, A.C. (2002). A centrosomal microtubule nucleation in higher plants. Int. Rev. Cytol. **220,** 257–289.

Shaw, S.L., Kamyar, R.M., and Ehrhardt, D.W. (2003). Sustained microtubule treadmilling in Arabidopsis cortical arrays. Science **300,** 1715–1718.

Sigrist, S., Jacobs, H., Stratmann, R., and Lehner, C.F. (1995). Exit from mitosis is regulated by *Drosophila* fizzy and the sequential destruction of cyclins A, B and B3. EMBO J. **14,** 4827–4838.

Smertenko, A., Saleh, N., Igarashi, H., Mori, H., Hauser-Hahn, I., Jiang, C.J., Sonobe, S., Lloyd, C.W., and Hussey, P.J. (2000). A new class of microtubule-associated proteins in plants. Natl. Cell Biol. **2,** 750–753.

Smith, L.G. (2002). Plant cytokinesis: Motoring to the finish. Curr. Biol. **12,** R206–R208.

Stals, H., Bauwens, S., Traas, J., Van Montagu, M., Engler, G., and Inze, D. (1997). Plant CDC2 is not only targeted to the pre-prophase band, but also co-localizes with the spindle, phragmoplast, and chromosomes. FEBS Lett. **418,** 229–234.

Strompen, G., El Kasmi, F., Richter, S., Lukowitz, W., Assaad, F.F., Jurgens, G., and Mayer, U. (2002). The *Arabidopsis* HINKEL gene encodes a kinesin-related protein involved in cytokinesis and is expressed in a cell cycle-dependent manner. Curr. Biol. **12,** 153–158.

Surana, U., Amon, A., Dowzer, C., McGrew, J., Byers, B., and Nasmyth, K. (1993). Destruction of the CDC28/CLB mitotic kinase is not required for the metaphase to anaphase transition in budding yeast. EMBO J. **12,** 1969–1978.

Uhlmann, F. (2001). Chromosome condensation: Packaging the genome. Curr. Biol. **11,** R384–R387.

Vandepoele, K., Raes, J., De Veylder, L., Rouze, P., Rombauts, S., and Inze, D. (2002). Genome-wide analysis of core cell cycle genes in *Arabidopsis*. Plant Cell **14,** 903–916.

Vasquez, R.J., Gard, D.L., and Cassimeris, L. (1999). Phosphorylation by CDK1 regulates XMAP215 function *in vitro*. Cell Motil. Cytoskeleton **43,** 310–321.

Vitrat, N., Cohen-Solal, K., Pique, C., Le Couedic, J.P., Norol, F., Larsen, A.K., Katz, A., Vainchenker, W., and Debili, N. (1998). Endomitosis of human megakaryocytes are due to abortive mitosis. Blood **91,** 3711–3723.

Wang, H., Zhou, Y., Gilmer, S., Whitwill, S., and Fowke, L.C. (2000). Expression of the plant cyclin-dependent kinase inhibitor ICK1 affects cell division, plant growth and morphology. Plant J. **24,** 613–623.

Wäsch, R., and Cross, F.R. (2002). APC-dependent proteolysis of the mitotic cyclin Clb2 is essential for mitotic exit. Nature **418,** 556–562.

Wasteneys, G.O. (2002). Microtubule organization in the green kingdom: Chaos or self-order? J. Cell Sci. **115,** 1345–1354.

Weingartner, M., Binarova, P., Drykova, D., Schweighofer, A., David, J.P., Heberle-Bors, E., Doonan, J., and Bogre, L. (2001). Dynamic recruitment of Cdc2 to specific microtubule structures during mitosis. Plant Cell **13,** 1929–1943.

Weingartner, M., Pelayo, H.R., Binarova, P., Zwerger, K., Melikant, B., De La Torre, C., Heberle-Bors, E., and Bogre, L. (2003). A plant cyclin B2 is degraded early in mitosis and its ectopic expression shortens G2-phase and alleviates the DNA-damage checkpoint. J. Cell Sci. **116,** 487–498.

Whittington, A.T., Vugrek, O., Wei, K.J., Hasenbein, N.G., Sugimoto, K., Rashbrooke, M.C., and Wasteneys, G.O. (2001). MOR1 is essential for organizing cortical microtubules in plants. Nature **411,** 610–613.

Willemsen, V., Wolkenfelt, H., de Vrieze, G., Weisbeek, P., and Scheres, B. (1998). The *HOBBIT* gene is required for formation of the root meristem in the *Arabidopsis* embryo. Development **125,** 521–531.

Yamano, H., Gannon, J., and Hunt, T. (1996). The role of proteolysis in cell cycle progression in *Schizosaccharomyces pombe*. EMBO J. **15,** 5268–5279.

Yang, J., and Kornbluth, S. (1999). All aboard the cyclin train: Subcellular trafficking of cyclins and their CDK partners. Trends Cell Biol. **9,** 207–210.

Zachariae, W., and Nasmyth, K. (1999). Whose end is destruction: Cell division and the anaphase-promoting complex. Genes Dev. **13,** 2039–2058.

Expression of a Nondegradable Cyclin B1 Affects Plant Development and Leads to Endomitosis by Inhibiting the Formation of a Phragmoplast
Magdalena Weingartner, Marie-Claire Criqui, Tamás Mészáros, Pavla Binarova, Anne-Catherine Schmit, Anne Helfer, Aude Derevier, Mathieu Erhardt, László Bögre and Pascal Genschik
Plant Cell 2004;16;643-657
DOI 10.1105/tpc.020057

This information is current as of June 13, 2012

References	This article cites 87 articles, 29 of which can be accessed free at: http://www.plantcell.org/content/16/3/643.full.html#ref-list-1
Permissions	https://www.copyright.com/ccc/openurl.do?sid=pd_hw1532298X&issn=1532298X&WT.mc_id=pd_hw1532298X
eTOCs	Sign up for eTOCs at: http://www.plantcell.org/cgi/alerts/ctmain
CiteTrack Alerts	Sign up for CiteTrack Alerts at: http://www.plantcell.org/cgi/alerts/ctmain
Subscription Information	Subscription Information for *The Plant Cell* and *Plant Physiology* is available at: http://www.aspb.org/publications/subscriptions.cfm

© American Society of Plant Biologists
ADVANCING THE SCIENCE OF PLANT BIOLOGY